International Journal of Engineering

Journal Homepage: www.ije.ir

Numerical Analyses of Manufacturing of an AA8111 Pin-shaped Bipolar Plate by Hot Metal Gas Forming

S. Esmaeili[a], S. J. Hosseinipour[*a], A. Shamsi-Sarband[b]

[a] *Research Center for Advanced Processes of Materials Forming, Babol Noshirvani University of Technology, Babol, Iran*
[b] *Department of Mechanical Engineering, Islamic Azad University-Sari Branch, Sari, Iran*

PAPER INFO

Paper history:
Received 17 February 2021
Received in revised form 10 July 2021
Accepted 13 July 2021

Keywords:
Aluminium Alloy
Hot Metal Gas Forming
Finite Elements Simulation
Bipolar Plates
Pin-type Pattern

ABSTRACT

In this paper, fabrication of a pin-shaped bipolar plate for a proton exchange membrane fuel cell, the deformation behavior of a thin 8111 aluminum alloy sheet by the hot metal gas forming (HMGF) process was investigated. The effect of gas pressure, forming time, pin diameter, pin height, and die fillet radius on the specimen profiles, as well as the thickness distribution were analyzed by finite element method using ABAQUS 6.10 software. In addition, experimental tests were performed to validate numerical outputs. The results indicated that the sheet-thinning rate sharply grew by the gas pressure exceeding 4 MPa. The specimens were cracked following decreasing the die fillet radius to 0.1 mm. Furthermore, the die filling rate was high at the beginning of forming time and then diminished gradually after 1000 s. Moreover, the thickness reduced sharply by augmenting the ratio of pin height to diameter to over 0.4. Finally, perfect specimens were produced in experiments, which verified the feasibility of fabricating a pin-shaped bipolar plate out of a thin AA8111 sheet by the HMGF process.

doi: *10.5829/ije.2021.34.08b.20*

1. INTRODUCTION

Nowadays, environmental issues and air pollution resulting from fossil fuels have led to a global attempt to replace traditional energy resources with clean ones. Fuel cells, which convert chemical potential energy to electrical power, can be considered among the best candidates. Bipolar plates play a remarkable role in the weight and price of the proton exchange membrane (PEM) fuel cell stacks [1, 2]. In this regard, metallic bipolar plates are widely used due to their low fabrication cost and desirable mechanical properties, [3]. Various methods, such as hydroforming, stamping, and rubber pad forming have already been investigated for forming metallic bipolar plates [4]. Koc and Mahabunphachai [5] used a two-stage hybrid process including hydroforming process and mechanical bonding to fabricate a multi-array micro-channel bipolar plate from the SS304 steel. These researchers showed that die filling increased with elevating internal pressure. Peng *et al.* [6] investigated the shape of the flow channel by hydroforming the metallic bipolar plate. They showed that geometric parameters, such as the fillet radius, as well as the depth and width of the flow channel, were important in the performance of bipolar plates. Liu *et al.* [7, 8] studied the feasibility of the rubber pad forming process to make the SS304 steel bipolar plate containing multi-array micro-flow channels. Hung *et al.* [9] studied micro-channel forming using high-pressure hydroforming. They indicated that the height to width ratio of a flow channel has an essential impact on the performance of a fuel cell. Belali-Owsia *et al.* [10] fabricated a pin-shaped bipolar plate from the SS304 steel sheet using three different methods of hydroforming, stamping, and hybrid hydroforming-stamping. Mohammadtabar *et al.* [11] examined the feasibility of a double-step hydroforming process to make a bipolar plate with a serpentine channel flow field. Ghadikolaee *et al.* [12] constructed metallic bipolar plates out of the SS316 steel utilizing the rubber pad forming process. They investigated the contribution

*Corresponding Author Institutional Email: j.hosseini@nit.ac.ir (S. J. Hosseinipour)

Please cite this article as: S. Esmaeili, S. J. Hosseinipour, A. Shamsi-Sarband, Numerical Analyses of Manufacturing of an AA8111 Pin-shaped Bipolar Plate by Hot Metal Gas Forming, International Journal of Engineering, Transactions IJE TRANSACTIONS B: Applications Vol. 34, No. 08, (August 2021) 1994-2001

of pressure, hardness, and thickness of a rubber pad in the maximum channel depth before fracture.

The applications of lightweight materials, such as aluminum alloys are being widely expanded in various industries, including the aerospace and transportation industries [13-17]. Aluminum alloys can be suitable as bipolar plates because of their desirable mechanical properties, corrosion resistance, thermal conductivity, and low electrical resistance. Lim *et al.* [18] studied the formability of AA1050 aluminum alloy to make a bipolar plate by the rubber pad forming process. They studied the influence of channel cross-sections on the velocity field of the bipolar plate. However, the formability of aluminum alloys at room temperature is limited, which can be resolved using high temperature forming processes [19, 20]. Therefore, Kwon *et al.* [21] used a warm progressive forming process to manufacture the micro-channel bipolar plates of AA5052 aluminum sheets. The latter researchers studied the effect of various parameters, namely forming speed and die temperature. In addition, Palumbo *et al.* [22] focused on the manufacturing of a bipolar plate from an AA6061 aluminum sheet using a warm hydroforming process. They analyzed both the channel profile and bipolar plate geometry by applying the finite element method (FEM). Taking advantage of the hot metal gas forming (HMGF) process, Esmaeili and Hosseinipour [23] experimentally studied the feasibility of forming a micro-channel bipolar plate out of AA8111 aluminum sheets with a serpentine channel flow field. Similarly, Kargar-Pishbijari *et al.* [24] experimentally investigated the fabrication of a micro-channel bipolar plate from an AA1070 aluminum alloy sheet with a thickness of 100 μm by the HMGF process.

As mentioned earlier, most research around the metallic bipolar plates has been performed on forming channel-shaped patterns through hydroforming, stamping, and rubber pad forming. The flow pattern of the bipolar plate has a significant impact on the fuel cell performance. The investigations showed that the performance of bipolar plates with a pin-shaped pattern did not decrease at high temperatures and the pressure drop was lower than with the channel-shaped flow field [6]. In this regard, little research has been conducted on the forming of pin-shaped bipolar plates. The fabrication of pin-shaped patterns from aluminum alloys is a considerable issue. Consequently, in this study, finite element simulations and experiments were carried out to evaluate the effects of various parameters on the deformation behavior of a thin AA8111 aluminum alloy sheet by the HMGF process to fabricate a pin-shaped bipolar plate.

2. MATERIALS AND METHODS

2. 1. Process description An AA8111 aluminum alloy sheet with 0.2 mm thickness was used for experimental tests. Figure 1 shows the HMGF equipment, which consists of an argon gas container, a temperature sensor, a temperature controller, a heating element, a gas pressure valve, as well as upper and lower dies. First, a circular blank was fixed between the upper and lower dies, and then at a specified temperature, constant gas pressure was applied for a specified duration to form the sheet on the die. Figure 2 indicates the pin-type pattern die used in the experimental tests, in addition to the geometric parameters, including pin diameter (S), pin height (H), flow path width (W), and die fillet radius (R). Table 1 presents the values of parameters analyzed in the present study.

Figure 3 demonstrates diverse conditions of the formed bipolar plates, including partially formed, cracked, and perfect specimens. The specimens were cut and mounted with resin to measure the profile and thickness of specimens as illustrated in Figure 4. Next, images were taken from the cut sections of specimens with a Dewinter optical microscope (Figure 5). Dewinter material plus software was also used to analyze the images.

Free bulging tests were performed to obtain the mechanical properties of the material at a specific temperature. For this purpose, two distinct pressures were applied and the dome height changes were measured at various time points [25]. Figure 6 depicts the free bulged sample and its parameters.

The work hardening is negligible at high temperatures. As a result, the material behavior can be expressed by Equation (1) [26];

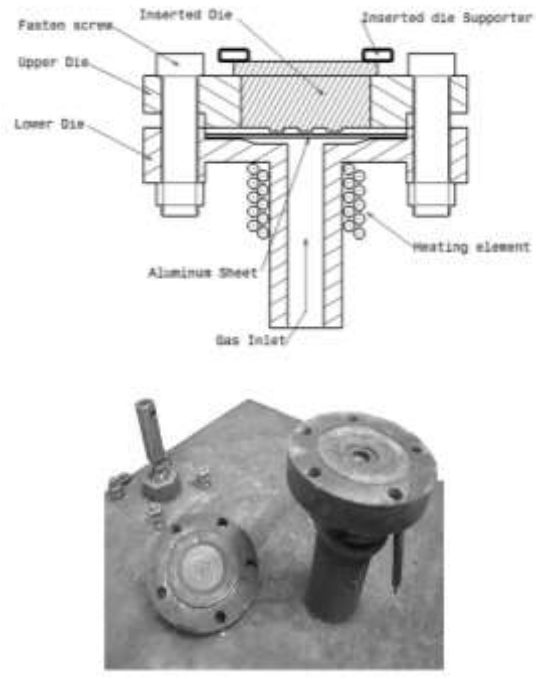

Figure 1. Experimental equipment

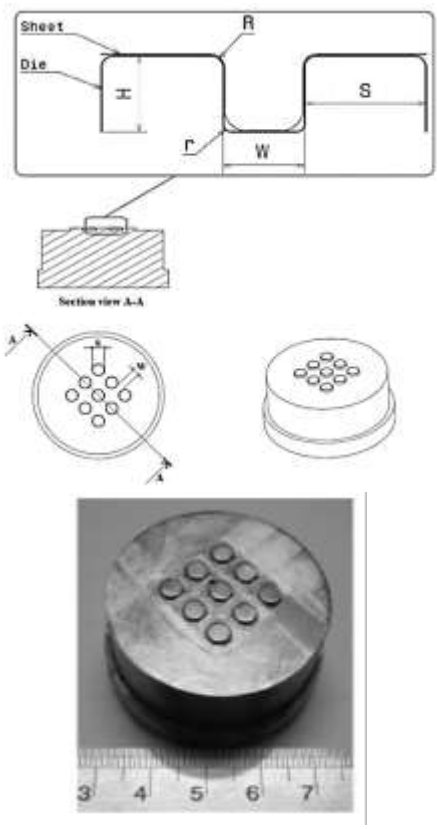

Figure 2. Pin-type pattern die and the parameters

TABLE 1. Range of investigated parameters and the material property at 500 °C

Forming Parameters	Range
Temperature (°C)	500
Pressure (MPa)	1-5
Forming Time (s)	100, 1000, 2000
Pin diameter, S (mm)	2-4
Flow path width, W (mm)	2
Fillet radius, R (mm)	0.1, 0.2, 0.3
Pine height, H (mm)	0.8, 1
H/S	0.2-0.5
Strain rate sensitivity exponent, m	0.08
Coefficient of strength, C (MPa)	14

$$\sigma = C\dot{\varepsilon}^{m} \quad (1)$$

where σ is the effective flow stress, $\dot{\varepsilon}$ denotes the effective strain rate, m refers to the strain rate sensitivity exponent, and C represents the coefficient of strength. The strain rate sensitivity exponent, m, can be determined by Equation (2);

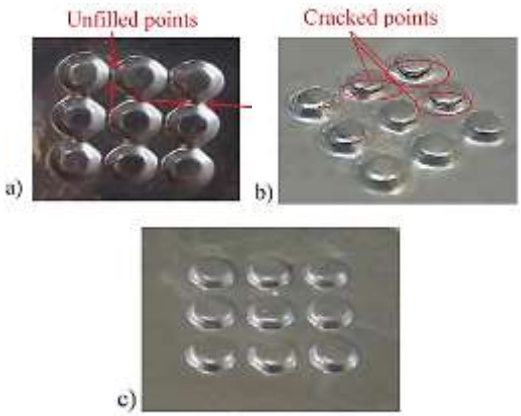

Figure 3. a) partially formed specimen, b) cracked specimen, and c) perfect specimen

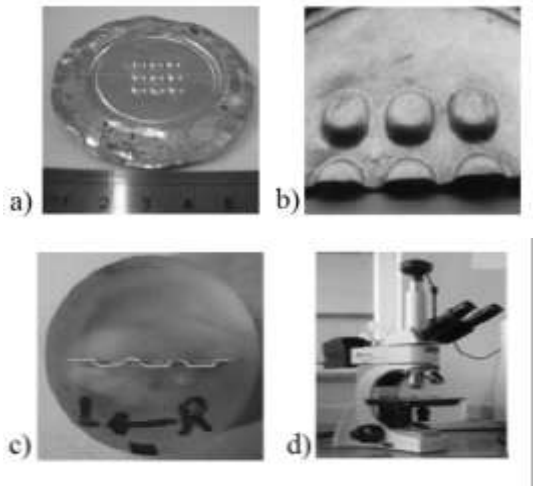

Figure 4. Preparation sequence to measure the profile and thickness of specimens

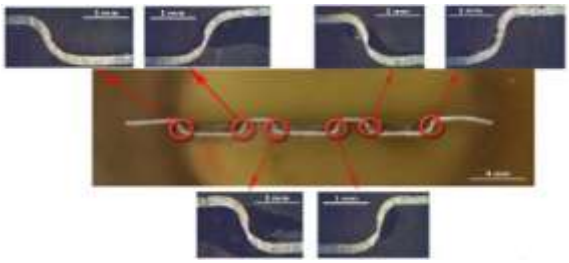

Figure 5. Cut a section of specimens

$$m = \frac{\ln(\frac{P_1}{P_2})}{\ln(\frac{t_1}{t_2})} \quad (2)$$

where t_1 and t_2 are the forming times to reach the same dome height at the constant pressures of P_1 and P_2, respectively. The stress state at the dome is equal to the biaxial tension. Therefore, the stress σ is calculated using Equation (3);

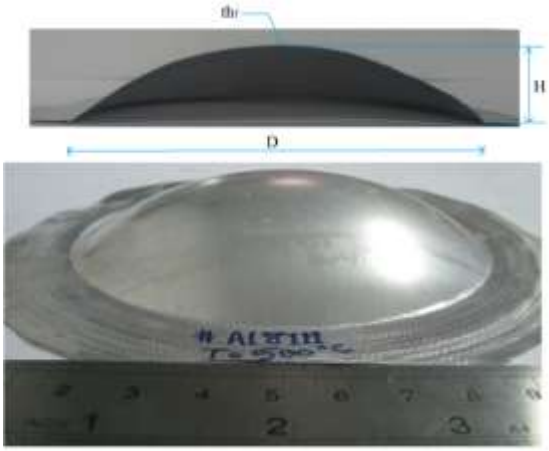

Figure 6. A free bulged specimen

$$\sigma = \frac{Pr}{2\,th_f} \quad (3)$$

where th_f denotes the thickness of sheet at the dome and r represents the dome radius calculated by Equation (4);

$$R = \frac{H^2+(\frac{D}{2})^2}{2H} \quad (4)$$

where D refers to the die diameter, and H is the dome height. The strain ε and strain rate $\dot{\varepsilon}$ can be calculated using Equations (5) and (6), respectively.

$$\varepsilon = ln\frac{th_f}{th_o} \quad (5)$$

$$\dot{\varepsilon} = \frac{d\varepsilon}{dt} \quad (6)$$

Table 1 represents the calculated values of C and m for the AA8111 at 500ºC.

2. 2. Numerical Simulation The finite element software ABAQUS 6.10 was used to simulate the process. Both the die and sheet were geometrically symmetric. Consequently, a quarter of the whole process was modeled (Figure 7). The die was defined as a discrete rigid body and the blank was modeled as a deformable shell element. An isotropic behavior was assumed for the material flow because deformation was performed at high temperature.

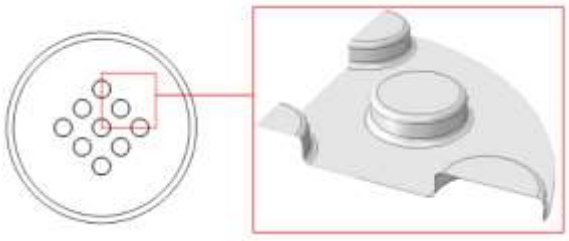

Figure 7. Die model in the finite element simulation

To enter the mechanical properties of the material into the software, a time-dependent deformation was described. Values of C and m at 500°C were also applied according to Table 1. Contact conditions were defined between the sheet and die surface [27, 28]. The die was fixed, and a constant uniform pressure was applied to the sheet during the forming process. The S4R element was used for meshing the blank model with the size of 0.02 mm based on the mesh convergence analysis depicted in Figure 8. **Error! Reference source not found.**According to the experimental results, the samples were cracked at the sheet thinning rate of 50% or more. Therefore, this level was considered as a failure limit in our finite element simulations. Figure 9 shows sheet deformation according to the geometry of the die in the simulation.

3. RESULTS AND DISCUSSION

3. 1. FEM Model Validation The simulation results were compared with the experimental tests to verify the accuracy of the FEM. To this aim, both the die filling profile and thickness distribution were examined. According to Figure 10, the die filling profile of the experimental method was highly matched with that of the simulation. Moreover, as could be seen in Figure 11, the thickness distributions of the formed plates were in agreement with each other in both experimental and simulation methods.

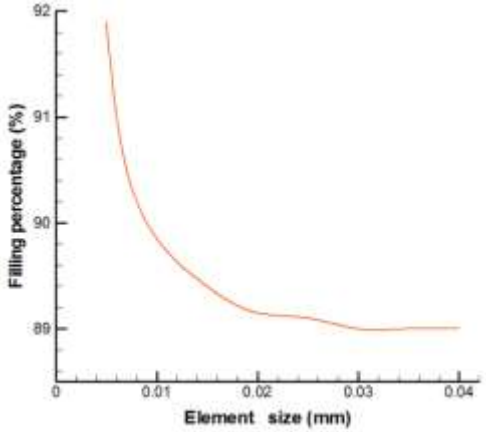

Figure 8. Mesh convergence diagram

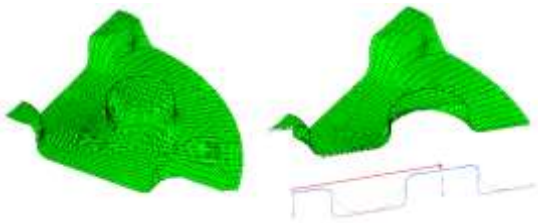

Figure 9. Deformed blank in the finite element simulation

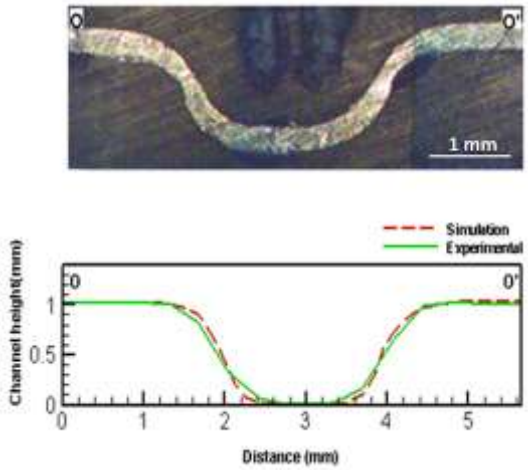

Figure 10 Die filling profile of a specimen (S=3mm, H=1mm, R=0.2mm, P=2MPa, t=1000s)

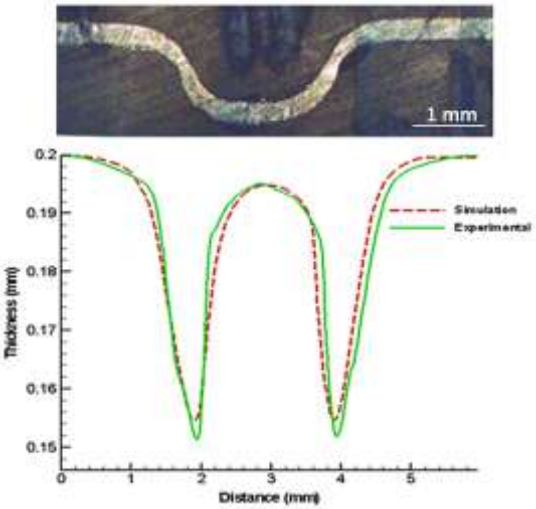

Figure 11. Thickness distribution of a specimen (S=3mm, H=0.8mm, R=0.2mm, P=1.6MPa, t=1000s)

3. 2. Effect of Forming Time Figure 12 shows the rate of die filling as a percentage at various time points during the forming process. It was observed that at constant pressure, the filling rate increased with time, however, this behavior was not always uniform. At the initial time points, a considerable amount of the filling occurred with the rest of the deformation occurring gradually. When the pressure was 2 MPa, the filling rate 100 and 2000 s after the beginning of the experiment was 73 and 82%, respectively. The filling rate declined due to the contact of sheet with die surface, and as a result of high friction between the hot die and the sheet, it took more time to be filled.

Figure 13 demonstrates the sheet thinning rate during the forming period. A high thinning rate was observed at the beginning of the process, whereas it continued at a slower rate during the rest of the experiment. Although the thinning rate was depicted for two different H/S values, it resulted in a similar thinning trend.

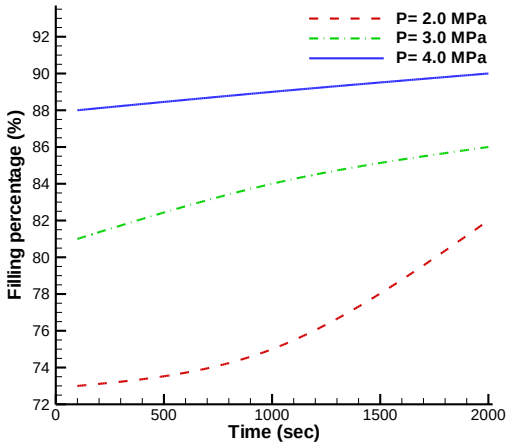

Figure 12. Effect of time on the filling rate (S=4mm, H=0.8mm, R=0.1mm)

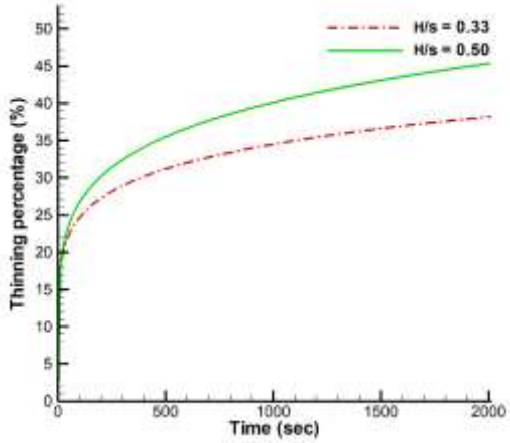

Figure 13. Effect of time on the thinning rate (R=0.2mm, P=2MPa)

3. 3. Effect of Gas Pressure Figure 14 indicates that the filling rate of the die cavity rises by elevating gas pressure. In order to obtain a perfect specimen, the sheet thinning rate should also be taken into consideration. According to Figure 15, the thinning rate grows by augmenting gas pressure. Moreover, the obtained results are shown for different H/S values. At lower pressures, the gas pushed the sheet to be drawn into the die cavity, and as a result, the thinning rate was not at critical values. By increasing the pressure, the sheet was forced to fill the corners of the die, and the thinning rate raised sharply. When H/S = 0.33 and P = 4 MPa, the thinning rate was 38%, which was below the threshold and acceptable. By increasing the pressure up to 5 MPa, the thinning rate reached 54%, which was beyond the failure limit.

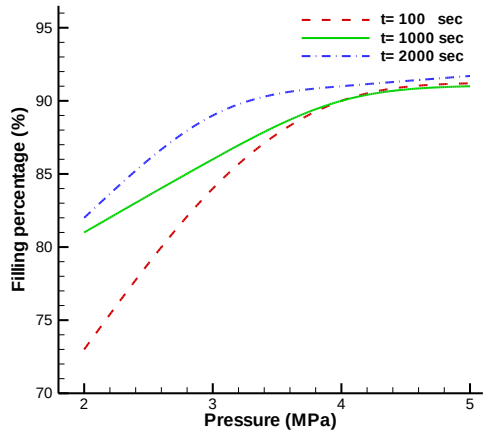

Figure 14. Impact of pressure on die filling rate (S=3mm, H=0.8mm, R=0.1)

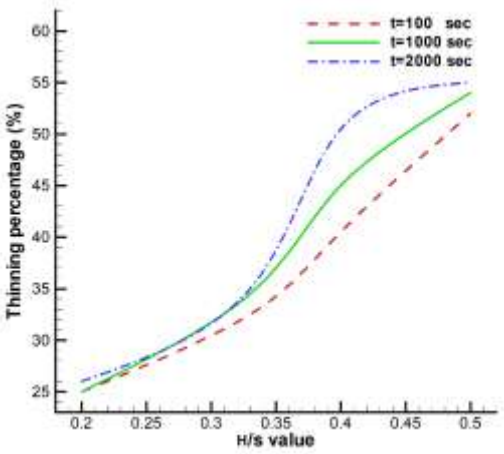

Figure 16. Effect of pressure on the thinning rate (R=0.1, t=2000s)

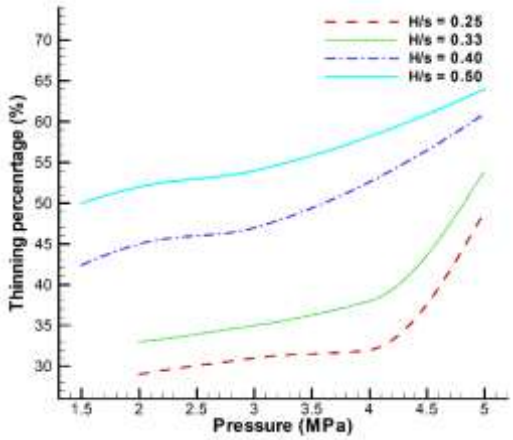

Figure 15. Effect of pressure on sheet thinning rate (R=0.1, t=2000s)

3. 4. Influence of Pin Height to Diameter Ratio (H/S) Figure 16 shows the effect of different H/S values on sheet thinning rate, at three different time points. It should be noted that an increase in the H/S value led to increase in the thinning rate. The latter trend was consistent throughout the whole study period. Moreover, by augmenting the H/S value, the sheet needed to stretch more to fill the die cavity. This phenomenon raised the extension ratio of the sheet and resulted in a higher thinning rate. When H/S varied as 0.2-0.4, the thinning rate raised from 25 to 44%, which was still within an acceptable range. However, by increasing the H/S to 0.5, the thinning rate reached 54% or higher, at which a crack was likely to appear in the specimen. Overall, the H/S value was revealed to be an essential parameter in the forming process.

Therefore, the H/S value of 0.5 was observed to be a critical value, at which the thinning rate elevated significantly and the sheet cracked during the forming process in a considerable number of experimental tests. This phenomenon can be explained by the contact area of the sheet and die during the forming process. As shown in Figure 17, at the same forming time, the first contact happened at the bottom of the die cavity for low H/S values. On the other hand, for high H/S values, it occurred on the vertical walls of the die before being drawn into the die cavity. Consequently, a considerable amount of the material was locked due to the friction in the contact area. Therefore, by continuing the forming process, the sheet was significantly prone to the experience of a high thinning rate.

3. 5. Effect of Fillet Radius (R) Figure 18 demonstrates the die filling rate at various R values. As R increased from 0.1 mm to 0.2 mm, the filing rate at all applied pressures sharply augmented. However, by elevating the amount of R from 0.2 mm to 0.3 mm, the filling rate did not change considerably implying that higher R could facilitate the drawing of the sheet material into the die cavity. Consequently, a higher rate of die cavity will be filled by the sheet. Furthermore, R has a crucial impact on the thinning of the formed specimens. According to the experimental observations, cracks in all cracked specimens occurred in areas where the sheets were in contact with the die fillet of the pin (as could be observed in Figure 3). Figure 19 indicates that by rising the value of R, the thinning rate declined. When R = 0.1

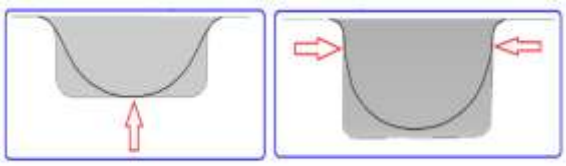

Figure 17. First contact area of sheet with die at a) low H/S value, and b) high H/S value

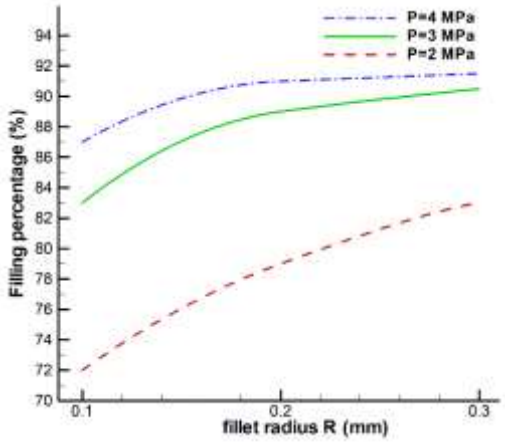

Figure 18. Influence of R on the filling rate (S=4mm, H=1mm, t=1000s)

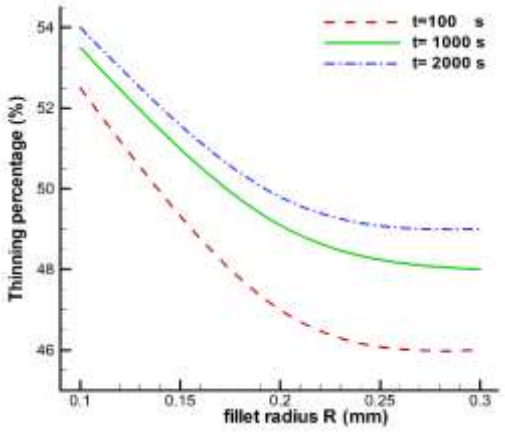

Figure 19. Effect of R on the thinning rate (S=2mm, H=1mm, P=3MPa)

mm, which was considered as a sharp fillet during all the forming periods, the thinning rate was higher than the critical limit (50%) and the samples were considered as cracked specimens. Finally, by selecting higher R values, such as 0.2 and 0.3 mm, the thinning rate diminished remarkably. However, this trend was not linear.

4. CONCLUSION

The current research studied the deformation behavior of a thin AA8111 alloy sheet by the HMGF process to fabricate a pin-shaped bipolar plate for PEM fuel cells. The effects of essential parameters, including forming time, gas pressure, die fillet radius, pin diameter, and pin height on die filling and sheet thinning rates were investigated.

It was found that gas pressure was an important parameter in the HMGF process. While the filling rate increased by applying high pressure, the thickness reduced. Altogether, when P > 4 MPa, not only the filling rate did not change considerably but also the thickness sharply decreased.

Furthermore, reducing the die fillet radius led to decreased sheet material flow to the die cavity and significantly increased sheet thinning. Noteworthy, the specimen was cracked in a die fillet radius of 0.1 mm, while the fillet radius of about 0.2 mm was acceptable.

The sheet thickness extremely reduced with the growth of the pin height to diameter ratio, which was due to an elevation in the extension ratio. Based on the obtained results, the pin height to diameter ratio of 0.33 and 0.4 generated the most desirable outcomes.

The deformation mechanism by the HMGF process is time-dependent. As a result, augmenting the forming time could increase the die filling rate. It is observed that the forming time of 1000-2000 s could be suitable for forming AA8111 bipolar plates.

5. ACKNOWLEDGMENTS

The authors acknowledge the funding support provided by Babol Noshirvani University of Technology through Grant number BNUT/370203/97.

6. REFERENCES

1. Hermann, A., Chaudhuri, T., Spagnol, P., "Bipolar plates for PEM fuel cells: A review", ***International Journal of Hydrogen Energy,*** Vol. 30, No. 12, (2005) 1297-1302. DOI: 10.1016/j.ijhydene.2005.04.016
2. Li, X., Sabir, I., "Review of bipolar plates in PEM fuel cells: Flow-field designs", ***International Journal of Hydrogen Energy,*** Vol. 30, No. 4, (2005) 359–371. DOI: 10.1016/j.ijhydene.2004.09.019
3. Weil, K. S., Xia, G., Yang, Z. G., Kim, J. Y., "Development of a niobium clad PEM fuel cell bipolar plate material", ***International Journal of Hydrogen Energy,*** Vol. 32, No. 16, (2007) 3724–3733. DOI: 10.1016/j.ijhydene.2006.08.041
4. Mehta, V., Cooper, J. S., "Review and analysis of PEM fuel cell design and manufacturing", ***Journal of Power Sources,*** Vol. 114, No. 1, (2003) 32–53. DOI: 10.1016/S0378-7753(02)00542-6
5. Koç, M., Mahabunphachai, S., "Feasibility investigations on a novel micro-manufacturing process for fabrication of fuel cell bipolar plates, Internal pressure-assisted embossing of micro-channels with in-die mechanical bonding", ***Journal of Power Sources,*** Vol. 172, No. 2, (2007) 725-733. DOI: 10.1016/j.jpowsour.2007.05.089
6. Peng, L., Lai, X., Hu, P., Ni, J., "Flow channel shape optimum design for hydroformed metal bipolar plate in PEM fuel cell", ***Journal of Power Sources,*** Vol. 178, No. 1, (2008) 223–230. DOI: 10.1016/j.jpowsour.2007.12.037
7. Liu, Y., Hua, L., "Fabrication of metallic bipolar plate for proton exchange membrane fuel cells by rubber pad forming", ***Journal of Power Sources,*** Vol. 195, No. 11, (2010) 3529–3535. DOI: 10.1016/j.jpowsour.2009.12.046
8. Liu, Y., Hua, L., Lan, J., Wei, X., "Studies of the deformation styles of the rubber-pad forming process used for manufacturing

metallic bipolar plates", ***Journal of Power Sources,*** Vol. 195, No. 24, (2010) 8177–8184. DOI: 10.1016/j.jpowsour.2010.06.078

9. Hung, J. C., Lin, C. C., "Fabrication of micro-flow channels for metallic bipolar plates by a high-pressure hydroforming apparatus", ***Journal of Power Sources,*** Vol. 206, (2012) 179-184. DOI: 10.1016/j.jpowsour.2012.01.112
10. Belali-Owsia, M., Bakhshi-Jooybari, M., Hosseinipour, S. J., Gorji, A., "A new process of forming metallic bipolar plates for PEM fuel cell with pin-type pattern", ***International Journal of Advanced Manufacturing Technology***, Vol. 77, Nos. 5-8, (2015) 1281–1293. DOI: 10.1007/s00170-014-6563-3
11. Mohammadtabar, N., Bakhshi-Jooybari, M., Hosseinipour, S. J., Gorji, A., "Feasibility study of a double-step hydroforming process for fabrication of fuel cell bipolar plates with slotted interdigitated serpentine flow field", ***International Journal of Advanced Manufacturing Technology***, Vol. 85, Nos. 1-4, (2016) 765–777. DOI: 10.1007/s00170-015-7960-y
12. Ghadikolaee, H. T., Elyasi, M., Khatir, F. A., Hosseinzadeh, M., "Experimental investigation of Fracture in rubber pad forming of bipolar plate's micro channels", ***Procedia Engineering,*** Vol. 207, (2017) 1647-1652. DOI: 10.1016/j.proeng.2017.10.1093
13. Oraon, M., Sharma, V., "Predicting Force in Single Point Incremental Forming by Using Artificial Neural Network", ***International Journal of Engineering, Transactions A: Basics***, Vol. 31, No. 1, (2018) 88-95. DOI: 10.5829/ije.2018.31.01a.13
14. Tabatabaeia, S. M. R, Alasvand Zarasvand, K., "Investigating the Effects of Cold Bulge Forming Speed on Thickness Variation and Mechanical Properties of Aluminium Alloys: Experimental and Numerical", ***International Journal of Engineering, Transactions C: Aspects,*** Vol. 31, No. 9, (2018) 1602-1608. DOI: 10.5829/ije.2018.31.09c.17
15. Rahmania, F., Seyedkashi, S. M. H., Hashemi, S. J., "Experimental Study on Warm Incremental Tube Forming of AA6063 Aluminum Tubes", ***International Journal of Engineering, Transactions C: Aspects***, Vol. 33, No. 9, (2020) 1773-1779. DOI: 10.5829/ije.2020.33.09c.11
16. Alijani Renani, H., Haji Aboutalebi, F., "Evaluation of Ductile Damage Criteria in Warm and Hot Forming Processes", ***International Journal of Engineering, Transactions A: Basics,*** Vol. 29, No. 10, (2016) 1441-1449. DOI: 10.5829/ije.2016.29.10a.15
17. Chausov, M., Pylypenko, A., Berezin, V., Volyanska, K., Maruschak, P., Hutsaylyuk, V., Markashova, L., Nedoseka, S., Menou, A., "Influence of dynamic non-equilibrium processes on strength and plasticity of materials of transportation systems", ***Transport***, Vol. 33, No. 1, (2018) 231-241. DOI: 10.3846/16484142.2017.1301549
18. Lim, S. S., Kim, Y., Kang, C., "Fabrication of aluminum 1050 micro-channel proton exchange membrane fuel cell bipolar plate using rubber-pad-forming process", ***International Journal of Advanced Manufacturing Technology,*** Vol. 65, Nos. 1-4, (2013) 231–238. DOI: 10.1007/s00170-012-4162-8
19. Li, Z., Qu, H., Chen, F., Wang, Y., Tan, Z., Kopec, M., Wang, K., Zheng, K., "Deformation Behavior and Microstructural Evolution during Hot Stamping of TA15 Sheets: Experimentation and Modelling", ***Materials*** Vol. 12, (2019), 223-236. DOI: 10.3390/ma12020223
20. Roohi, A. H., Hashemi, S. J., Allahyari, M., "Hot metal gas forming of closed-cell aluminum foam sandwich panels", ***Transactions of the Indian Institute of Metals,*** Vol. 73, (2020) 2231-2238. DOI: 10.1007/s12666-020-02027-2
21. Kwon, H. J., Jeon, Y. P., Kang, C. G., "Effect of progressive forming process and processing variables on the formability of aluminum bipolar plate with microchannel", ***International Journal of Advanced Manufacturing Technology,*** Vol. 65, Nos. 5-8, (2013) 681–694. DOI: 10.1007/s00170-012-4033-3
22. Palumbo, G., Piccininni, A., "Numerical–experimental investigations on the manufacturing of an aluminum bipolar plate for proton exchange membrane fuel cells by warm hydroforming", ***International Journal of Advanced Manufacturing Technology,*** Vol. 69, Nos. 1-4, (2013) 731–742. DOI: 10.1007/s00170-013-5047-1
23. Esmaeili, S., Hosseinipour, S. J., "Experimental investigation of forming metallic bipolar plates by hot metal gas forming (HMGF)", ***SN Applied Science,*** Vol. 1, No. 2, (2019) 187-191. DOI: 10.1007/s42452-019-0202-4
24. Kargar-Pishbijari, H., Hosseinipour, S. J., Jamshidi Aval, H., "A novel method for manufacturing microchannels of metallic bipolar plate fuel cell by the hot metal gas forming process", ***Journal of Manufacturing Processes,*** Vol. 55, (2020) 268-275. DOI: 10.1016/j.jmapro.2020.04.040
25. Giuliano, G., Franchitti, S., "On the evaluation of superplastic characteristics using the finite element method", ***International Journal of Advanced Manufacturing Technology,*** Vol. 47, Nos. 3-4, (2007) 471-476. DOI: 10.1016/j.ijmachtools.2006.06.009
26. Giuliano, G., Franchitti, S., "The determination of material parameters from superplastic free-bulging tests at constant pressure", ***International Journal of Machine Tools and Manufacture,*** Vol. 48, Nos. 12-13, (2008) 1519-1522. DOI: 10.1016/j.ijmachtools.2008.05.007
27. Shamsi-Sarband, A., Hosseinipour, S. J., Bakhshi-Jooybari, M., Shakeri, M., "The effect of geometric parameters of conical cups on the preform shape in two-stage superplastic forming process', ***Journal of Materials Engineering and Performance,*** Vol. 22, (2013), 3601-3611. DOI: 10.1007/s11665-013-0636-6
28. Hojjati, M., Zoorabadi, M., Hosseinipour, S. J., "Optimization of superplastic hydroforming process of Aluminum alloy 5083", ***Journal of Materials Processing Technology,*** Vol. 205, (2008), 482-488. DOI: 10.1016/j.jmatprotec.2007.11.208

Persian Abstract

چکیده

در این مقاله تغییر شکل یک ورق نازک از آلیاژ آلومینیوم ۸۱۱۱ AA برای ساخت صفحه دو قطبی برای پیل سوختی PEM با الگوی پین شکل با استفاده از فرایند شکل‌دهی داغ فلز با گاز (HMGF) بررسی شد. اثرات فشار گاز، زمان شکل‌دهی، قطر پین، ارتفاع پین و شعاع فیلت، بر پروفیل و توزیع ضخامت نمونه‌ها با استفاده از روش اجزای محدود با استفاده از نرم افزار ABAQUS 6.10 مورد مطالعه قرار گرفت. درستی شبیه‌سازی اجزای محدود با آزمایشات تجربی تایید گردید. نتایج نشان می‌دهد که با افزایش فشار گاز بیش از ۴ مگاپاسکال، سرعت نازک شدن به شدت افزایش یافت. با کاهش شعاع فیلت به کمتر از ۰/۲ میلی متر، نمونه شکسته شد. با افزایش زمان شکل‌دهی به بیش از ۱۰۰۰ ثانیه، نرخ افزایش پرشدگی کم می‌شود. علاوه بر این، کاهش ضخامت با افزایش نسبت ارتفاع به قطر پین به بیش از ۰/۴ به شدت افزایش یافت. سرانجام ، نمونه‌های کاملی در آزمایشات تولید شد که امکان ساخت صفحات دو قطبی نازک پین شکل از آلیاژ آلومینیوم ۸۱۱۱ AA را با فرآیند HMGF تأیید می‌کند.